Role of *cis*-1,4-cyclohexanedicarboxylic acid in the regulation of the structure and properties of a poly(butylene adipate-*co*-butylene 1,4-cyclohexanedicarboxylate) copolymer†

Fei Liu, Jia Qiu, Jinggang Wang, Junwu Zhang, Haining Na* and Jin Zhu*

A unique non-planar ring structure 1,4-cyclohexanedicarboxylic acid (CHDA) is introduced to synthesize a poly(butylene adipate-*co*-butylene 1,4-cyclohexanedicarboxylate) (PBAC) copolyester. The impact of the stereochemistry of CHDA on the structure and properties of PBAC, especially the role of *cis*-CHDA in tuning the thermal, tensile and elastic properties of PBAC is explored in depth. Instead of considering PBAC as a diblock random copolymer consisting of poly(butylene adipate) (PBA) and poly(butylene 1,4-cyclohexanedicarboxylate) (PBC), our results reveal that PBAC can be considered as a random copolymer consisting of actually three blocks, namely PBA, a PBC unit with only *trans*-CHDA (*trans*-PBC), and PBC unit with only *cis*-CHDA (*cis*-PBC). The role of *cis*-CHDA is found to be rigid which initiates a high modulus and strength, and soft which results in a decreased melting temperature and increased elongation at break and elasticity.

Introduction

1,4-Cyclohexanedicarboxylic acid (CHDA) is a unique aliphatic monomer with a non-planar ring structure. The influence of CHDA on the structure and properties has been demonstrated in many types of polymers such as polyesters,[1–8] polyamides,[9] polycarbonates[10] and thermoplastic elastomers.[11–13] Although people have realized that the six-membered CHDA moiety is versatile in terms of stereochemistry, namely, it has two isomers including *trans*-CHDA and *cis*-CHDA (Scheme 1),[2,11,14–17] previous research has focused on only *trans*-CHDA in order to obtain polymers with a high melting temperature,[16] tensile modulus[10,18] or better gas barrier properties.[5,13,19] There is a very small amount of work making full use of the *cis*-CHDA.[20]

Comparing with the *trans*- isomer which tends to reside in a chair conformation,[14] the *cis*-one prefers boat conformation (Scheme 1).[15] Thus the structure of *trans*-CHDA is regular while that of its *cis*-counterpart is irregular.[16] As a result, *trans*-CHDA is more likely to form stable crystalline while the *cis*-one introduces "kinks" to the molecular chain and hinders the crystallization of its *trans*-counterpart.[2,16] In order to take good advantage of the *cis*-CHDA, recently, we reported the impact of CHDA to a thermoplastic elastomer, and revealed the "elastic" feature of this structure by changing its stereochemistry.[21] Subsequently, we were able to obtain a soft-segment free polyester elastomer with high performance by merely increasing the *cis*-CHDA amount in a simple polyester poly(butylene 1,4-cyclohexanedicarboxylate) (PBC).[22] These findings inspire us that the *cis*-CHDA has huge potential in terms of obtain polymers with very different properties. Therefore, we take a step forward in current work and incorporate CHDA, especially the *cis*-isomer into a copolyester system poly(butylene adipate-*co*-butylene 1,4-cyclohexanedicarboxylate) (PBAC).

PBAC is a novel copolyester containing both linear aliphatic chain and cyclic aliphatic moiety.[23,24] It has properties that are quite different from those of copolyesters with only linear

Ningbo Key Laboratory of Polymer Materials, Ningbo Institute of Materials Technology and Engineering, Chinese Academy of Sciences, 1219 Zhongguan West Road, Ningbo, Zhejiang 315201, P.R. China. E-mail: jzhu@nimte.ac.cn; nahaining@nimte.ac.cn; Fax: +86-574-86685925; Tel: +86-574-86685925

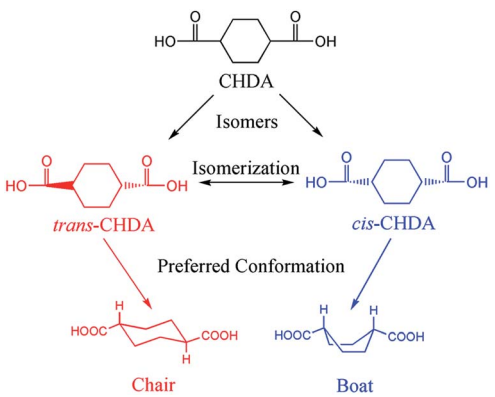

Scheme 1 Structure of CHDA isomers and their preferred conformations.[14,15]

aliphatic chain,[25–30] such as poly(butylene succinate-*co*-butylene adipate) (PBSA),[26,30] or those with both aliphatic chain and aromatic ring moiety, such as poly(butylene adipate-*co*-butylene terephthalate) (PBAT)[31,32] and poly(butylene adipate-*co*-butylene 2,5-furandicarboxylate) (PBAF).[33,34] The presence of the cyclic aliphatic moiety CHDA, renders the copolymer with excellent thermal stability even better than PBAT,[23] and potential biodegradability like PBSA.[23,26] More importantly, the structure and properties of PBAC copolymer can be tuned not only by changing the compositions of CHDA and adipic acid (AA), but also by varying the stereochemistry of CHDA.[23] Therefore, in current work, the influence of CHDA, especially *cis*-CHDA, as well as its co-monomer AA on the composition and structure of PBAC copolymer will be fully investigated. More importantly, the roles of *cis*-CHDA and AA they play in tuning the thermal, tensile as well as elastic properties of PBAC copolymer will be discussed and displayed in detail.

Results and discussion

Structure and compositions of PBAC copolymers

PBAC copolymers with different compositions (*i.e.* PBC amount) and CHDA *cis*/*trans* ratios are successfully obtained. In the first place, to investigate the influence of PBC amount on the properties of the PBAC copolymers, five PBAC samples with PBC contents in the final products ranging from 50 to 90 mol% are obtained. In these series, *trans*-CHDA is used as starting material so that the *cis*/*trans* ratios of CHDA in the final products are kept at 10/90. Subsequently, in order to evaluate the impact of *cis*-CHDA on the properties of PBAC copolymers, another two PBAC samples synthesized with *mix*-CHDA and *cis*-CHDA as starting materials are obtained, and the *cis*/*trans* ratios of CHDA in these two final products are 50/50 and 70/30, respectively. The PBC amount in these two samples is kept at a constant value of 80 mol%. Finally, two homopolymers (*i.e.* PBA and PBC) are also produced for comparation.

Six PBAC copolymers with *trans*-CHDA as starting material are denoted as PBAC-*x*, where *x* stands for the molar ratio of PBC and is in the range of 50 to 90. For example, PBAC-50 means that the polymer contains 50 mol% of PBC and the ratio of *trans* isomer of CHDA is 90 mol%. Another two PBAC copolymers with *mix*-CHDA and *cis*-CHDA as starting materials are named as PBAC-80-*mix* and PBAC-80-*cis*. These two PBAC copolymers contains 80 mol% of PBC and the ratios of *trans* isomer of CHDA are 60 and 30 mol% respectively.

Fig. 1 shows the ^{1}H NMR spectra of PBA and PBC homopolymers as well as that of a typical PBAC copolymer (PBAC-50). All peaks varying in chemical shifts can be attributed to correspondent protons in the products.[22,23] The compositions of the PBAC copolymers are calculated based on the integration ($I_{e\text{-}cis}$, $I_{e\text{-}trans}$ and I_a) of three peaks located at $\delta = 2.47$ ppm (e-*cis*), 2.33 ppm (e-*trans*) and 2.28 ppm (a) (Fig. 1). These three peaks can be assigned to the protons in –C*H*– in *cis*-CHDA, *trans*-CHDA and –C(O)CH_2– in butylene adipate unit, respectively. It is worth noting that, the peak for the protons in –OCH_2– unit in PBA homopolymer locates at $\delta = 4.04$ ppm (c′), while it shifts to $\delta = 4.09$ ppm (c) in PBAC copolymer and merges with the peak of

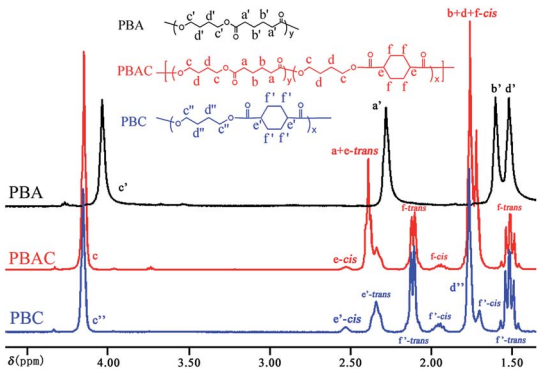

Fig. 1 ^{1}H NMR (400 MHz, $CDCl_3$) spectra of PBA, PBC and a typical PBAC copolymer (PBAC-50).

protons in –OCH_2– unit in PBC. The molar percentage of PBC as well as the ratio of *trans*-CHDA isomer in the copolymer are calculated according to eqn (1) and (2) respectively.[21,22] The correspondent results are summarized and collected in Table 1.

$$\text{PBC mol\%} = \frac{I_{e-cis} + I_{e-trans}}{I_{e-cis} + I_{e-trans} + I_a} \quad (1)$$

$$\textit{trans}\text{-CHDA mol\%} = \frac{I_{e\text{-}trans}}{I_{e\text{-}cis} + I_{e\text{-}trans}} \quad (2)$$

It is clearly showed in Table 1 that all samples have comparable high molecular weight (M_n) and the molecular weight distributions (M_w/M_n) are in the range of 2.3 to 3.5. The compositions (PBC and PBA molar percentage) of all final products are in good agreement with the feed ones. More importantly, certain amount of deviation of final *cis*/*trans* ratios to the feed ones is observed for all samples. For example, samples with *trans*-CHDA (99 mol%) as starting material have ratios of *trans*-CHDA in the range of 81 to 92 mol%, while samples with *mix*-CHDA (*cis*/*trans* 50/50) and *cis*-CHDA (97 mol%) have ratios of *trans*-CHDA of 58 and 28 mol% respectively. This phenomenon is due to the fact that *cis*/*trans* isomers

Table 1 Compositions and molecular weights of PBA, PBC and PBAC copolymers[a]

Sample	PBC (mol%)	PBA (mol%)	*trans*-CHDA (mol%)	M_n	M_w/M_n
PBA	0	100	0	42 000	2.7
PBAC-50	49	51	84	44 000	3.5
PBAC-60	64	36	81	36 000	3.3
PBAC-70	73	27	92	40 000	2.3
PBAC-80	80	20	88	36 000	2.3
PBAC-90	93	7	91	42 000	2.6
PBAC-80-*mix*	81	19	58	40 000	2.5
PBAC-80-*cis*	82	18	28	43 000	2.6
PBC	100	0	88	33 000	2.5

[a] The compositions are calculated from ^{1}H NMR and molecular weight (M_n) and molecular weight distribution (M_w/M_n) are determined by GPC in $CHCl_3$.

of CHDA have a thermodynamic equilibrium of 34/66.[17] The isomerization reaction between *cis* and *trans* isomers are inevitable under high temperature once it is not in the balanced state (Scheme 1).[22] The observed deviation is in the range of 7–18% for samples with *trans*-CHDA as starting material, while those for samples with *mix*-CHDA and *cis*-CHDA are 8 and 25%, respectively. Nonetheless, we are able to obtain a series of PBAC samples with different compositions as well as CHDA *cis*/*trans* ratios.

It is worth noting that the sequence, number-average length of units and randomness of copolymer synthesized from BDO, AA and a third monomer can be obtained according to the results from ^{1}H NMR analysis.[33,34] For example, Wu and coauthors[34] synthesized PBAF copolymer with 2,5-furandicarboxylic acid as a third monomer. They were able to distinguish three sequences according to the chemical shifts of protons in –OCH_2– unit due to the conjugation effect resulting from the aromatic furan ring. The number-average unit length as well as the degree of randomness can be calculated accordingly. However, for PBAC copolymer, the third monomer is the non-planar aliphatic ring structure CHDA, which does not show conjugation effect like the aromatic furan ring.[33,34] Therefore, there is only one single peak for protons in –OCH_2– unit in all possible sequences (CBC, ABA and ABC), locating at $\delta = 4.09$ ppm (c).[22,23] Consequently, the sequence, number-average length of PBC and PBA unit as well as the degree of randomness are unable to determine from ^{1}H NMR results. We then turned to ^{13}C NMR spectra and found that for all PBAC copolymers, only PBAC-50 shows distinguishable peaks in the range of 173.0 to 175.5 ppm (Fig. S1†), which could be assigned to different sequences in the PBAC copolymer (see ESI for detailed analysis†). The calculated number-average lengths for PBA and PBC units in PBAC-50 are 1.62 and 2.24, respectively. The degree of randomness is 1.06, which is very close to 1, suggesting that this copolymer is a random copolymer (Table S2†). This result further implies that for the series of PBAC samples obtained in this work, with the increase of PBC amount, the number-average length for PBC will be greater than 2.24, while that of PBA will be smaller than 1.62.[34] As a result, the influence of PBA unit on the chemical shift of carbonyl carbon in PBC unit becomes negligible. Therefore, it is unable to tell the differences among different sequences in the PBAC copolymers in the ^{13}C NMR spectra when PBC amount is higher than 50%. Nevertheless, it is reasonable to conclude that PBAC samples are random copolymers and the number-average length of PBC unit is longer than that of PBA unit.

Thermal properties of PBAC copolymers

The thermal transitions and stability of PBAC copolymers were investigated by DSC and TGA characterizations. Fig. 2 shows the DSC curves of PBA and PBC homopolymers as well as PBAC copolymers with different compositions. The results are summarized in Table 2. Berti and coauthors[23] have discussed in detail about the glass transition temperature (T_g) of a series of PBAC copolymers according to the Fox equation, therefore, our work here will only focus on the influence of composition as

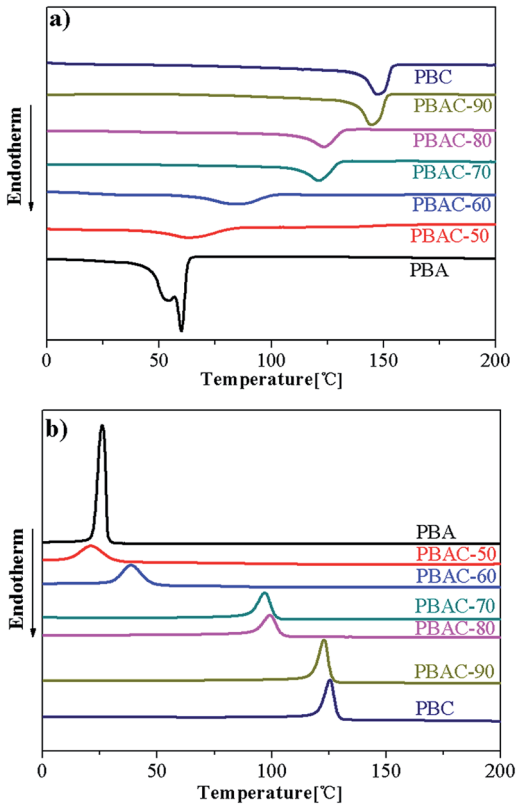

Fig. 2 DSC curves for PBA, PBC and PBAC copolymers with different compositions: (a) second heating and (b) cooling scans.

well as the stereochemistry of CHDA on the melting temperature T_m and the crystallization temperature T_c of the PBAC copolymers. Obviously, the T_m and T_c of all PBAC copolymers are within the range of those of PBA and PBC homopolymers. And with the increasing amount of PBC from 50 to 90%, both T_m and T_c increase gradually. On the other hand, decreasing the amount of *trans*-CHDA, namely increasing the amount of *cis*-CHDA results in amorphous copolymers with neither T_m nor T_c as showed in Fig. 3.

Table 2 Thermal properties of PBA, PBC and PBAC copolymers[a]

Sample	T_m (°C)	ΔH_m (J g^{-1})	T_c (°C)	χ_c (%)	$T_{5\%}$ (N_2) (°C)
PBA	54, 60	60	26	44.4	374
PBAC-50	63	18	21	14.2	356
PBAC-60	85	17	39	13.9	362
PBAC-70	121	17	97	12.9	375
PBAC-80	123	19	99	15.0	378
PBAC-90	145	26	123	20.2	378
PBAC-80-*mix*	None	None	None	None	379
PBAC-80-*cis*	None	None	None	None	365
PBC	147	24	125	19.3	382

[a] Melting temperature T_m, melting enthalpy ΔH_m and degree of crystallinity χ_c are determined from second heating scan of DSC curves and the crystallization temperature T_c is determined from the cooling scans of DSC curves, the temperature at 5% weight loss $T_{5\%}$ is determined by TGA in N_2 atmosphere.

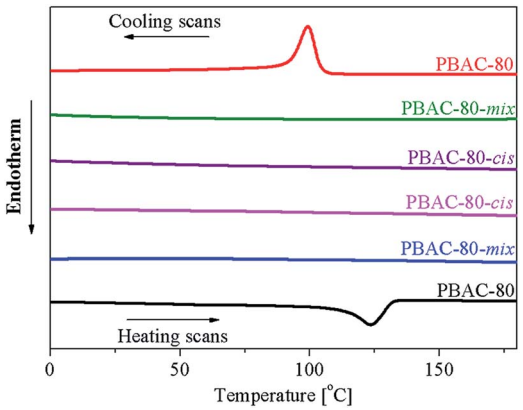

Fig. 3 DSC curves for PBAC copolymers containing 80 mol% PBC with different amount of *trans*-CHDA.

Wide angle X-ray diffraction (WAXD) analysis (Fig. 4) indicates that the crystal lattices of PBA and PBC homopolymers are totally different from each other. PBA molecules crystallize with a monoclinic crystal lattice correspondent to its α form,[29,35] which is in good agreement with its double melting peak observed in DSC analysis due to a fusion-recrystallization process.[22,36] While PBC molecules crystallize with a triclinic crystal lattice similar to that of PBT in α form.[31,37] When it comes to the PBAC copolymers, all samples show relatively intense diffraction peaks resembling those of PBC over the whole compositional range from 50 to 90%. This observation reveals that the crystalline phase for all PBAC copolymers with different compositions is merely PBC crystalline phase,[23] suggesting that only PBC part can crystallize in the copolymer when PBC amount is higher than 50%, and PBA is in the amorphous region. Furthermore, since it has been demonstrated in previous section that for all PABC copolymers with PBC amount higher than 50%, the number-average length of PBA unit is less than 1.62, PBA is unable to crystallize with such short chain length. Actually, the number-average length of PBA unit may have to reach 6.83 to initiate effective crystallization of itself.[34]

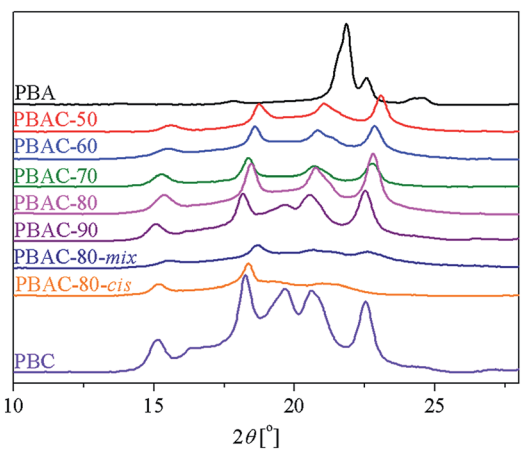

Fig. 4 Wide angle X-ray diffraction (WAXD) patterns of PBA, PBC and PBAC copolymers.

Based on the aforementioned results from WAXD, the T_m of the PBAC copolymers is actually from the crystallized PBC part. Therefore, the decreasing of T_m for the PBAC copolymers from 145 to 63 °C is due to the depression effect of the non-crystalline PBA on the PBC crystalline when the amount of PBA increases from 10 to 50%. This depression effect in a random copolymer was well investigated by Flory.[38] The relationship between T_m of the PBAC copolymer ($T_{m,\ PBAC}$) and the equilibrium T_m of the PBC homopolymer ($T^{\circ}_{m,PBC}$) can be described with the Flory eqn (3):[39]

$$\frac{1}{T_{m,PBAC}} = \left(\frac{R}{\Delta H_u}\right) \ln p + \frac{1}{T^{\circ}_{m,PBC}} \quad (3)$$

where R is the universal gas constant, p is the molar fraction of the crystallizable PBC unit and ΔH_u is the enthalpy of fusion per crystallizable repeating PBC unit.

According to the Flory equation, there is a linear relationship between ln p and $1/T_{m,PBAC}$. Noted that, p is the molar fraction of only the crystallizable PBC unit. While in the PBC part, only those formed with *trans*-CHDA are crystallizable,[22] thus we should also exclude the PBC part containing *cis*-CHDA for the calculation of p. Fig. 5 shows the plot of Flory equation and linear fitting for PBAC copolymers with different amount of PBC. A higher correlation coefficient (R^2) is obtained when *cis*-CHDA is excluded for the calculation of p (Fig. 5a, $R^2 = 0.994$), while a lower value is observed if all CHDA isomer regardless of its stereochemistry is included for the calculation of p (Fig. 5b, $R^2 = 0.960$). Therefore, both *cis*-CHDA and PBA should be considered as non-crystallizable parts in the PBAC copolymer. More importantly, this result strongly implies that the PBAC copolymer can be described as a random triblock copolymer which consists with three blocks: *trans*-PBC, *cis*-PBC and PBA. Only the *trans*-PBC part can form stable crystalline, while the presence of *cis*-PBC and PBA will suppress the crystallization of *trans*-PBC. Therefore, increasing amount of PBA in the copolymer results in decreased T_m. While more amount of *cis*-CHDA significantly reduces the crystallization ability of *trans*-CHDA,[22] giving amorphous PBAC copolymers, such as PBAC-80-*mix* and PBAC-80-*cis*. Interestingly, the PBC homopolymer therefore can be considered as a random "diblock copolymer" consists with *trans*-PBC and *cis*-PBC.[40] Applying Flory equation and linear fitting for the PBC series based on our previous data[22] give a correlation coefficient (R^2) of 0.998 (Fig. 5c), indicating that it is reasonable to describe PBC as a random "diblock copolymer".

In addition, the thermal stability of PBAC copolymers decreases with the increasing amount of PBA. The $T_{5\%}$ decreases all the way from 378 to 356 °C when the amount of PBA increases from 10 to 50%. This is due to the fact that the linear aliphatic chain is more vulnerable to thermal decomposition compared with cyclic aliphatic chain.[16] On the other hand, incorporation of more amount of *cis*-CHDA to the PBAC copolymer results in reduced thermal stability. The $T_{5\%}$ decreases from 378 to 365 °C with the increasing of *cis*-CHDA from 12 to 72%. This trend is not observed in PBC polymer,[22] probably due to the existence of linear aliphatic chain in PBAC copolymer.

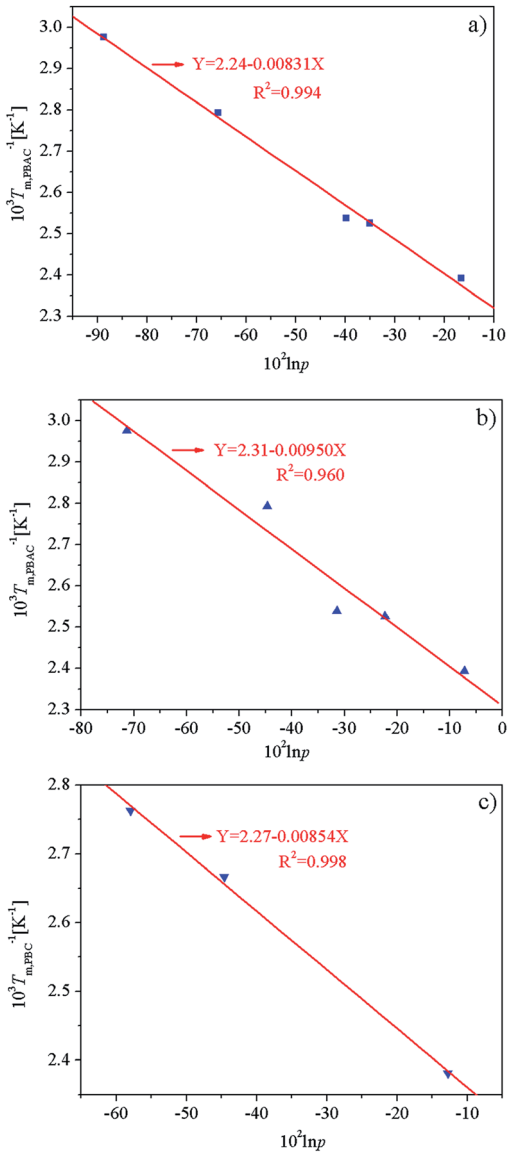

Fig. 5 Plot of Flory equation (blue dots) and linear fitting (red lines) for (a) excluding and (b) including *cis*-CHDA in PBAC copolymers with different amount of PBC and (c) in PBC homopolymer with different *cis*/*trans* ratio of CHDA.[22]

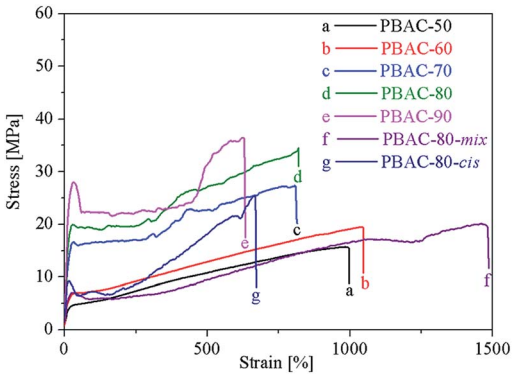

Fig. 6 Tensile strain–stress curves of PBAC copolymers.

Tensile properties of PBAC copolymers

The structure and thermal properties of PBAC copolymers experience sharp change when varying PBC amount and *cis*/*trans* ratio of CHDA. It is predictable that the tensile properties of these PBAC copolymers will also have significant variation accordingly. Fig. 6 shows the strain-stress curves of all PBAC copolymers and the relevant tensile properties are collected in Table 3.

Firstly, with the increasing amount of PBA from 10 to 50%, PBAC copolymers have substantial decreasing of tensile modulus E from 291 to 23 MPa, and tensile strength σ_t from 43 to 16 Mpa, respectively. While the elongation at break ε_b shows an increasing trend from 635 to over 1000% at the same time. These results indicate that the effect of PBA amount on the tensile properties of PBAC copolymer is similar to that of polyether soft segment on the tensile properties of thermoplastic poly(ether-ester) elastomer.[20,41] The amorphous PBA aliphatic chain plays a role similar to that of a polyether linkage in terms of tuning the tensile properties of semicrystalline polyesters. Secondly, considering the change of *cis*-CHDA from 12 to 72%, the E and σ_t of the PBAC copolymers show minimum values of 52 and 19 MPa, respectively, when the amount of *cis*-CHDA is 42% (sample PBAC-80-*mix*). While simultaneously the ε_b has a maximum value of approximately 1500%. These results are surprisingly the same as in the PBC homopolymer,[22] indicating the significant impact of *cis*-CHDA on the tensile properties of polymers containing the unique non-planar ring structure, even in the present of a relatively soft aliphatic PBA chain.

Since in the previous section it has been concluded that PBAC copolymers can be considered as triblock copolymers consist with three blocks: *trans*-PBC, *cis*-PBC as well as PBA. The results in the tensile analysis further demonstrate the different roles of these three blocks. The crystallizable *trans*-PBC part takes the position of a hard segment, providing the copolymer with high modulus, melting temperature as well as thermal stability. The short PBA aliphatic chain part, on the other hand, plays a role as soft segment, resulting in increasing of ε_b and decreasing of strength and melting temperature. What's more important, the *cis*-PBC part displays features of both hard and soft segments. It not only causes improved modulus and

Table 3 Tensile properties of PBA, PBC and PBAC copolymers[a]

Sample	E (Mpa)	σ_t (Mpa)	ε_b (%)	σ_y (Mpa)	ε_y (%)
PBA	220 ± 26	49 ± 1	1977 ± 88	18 ± 1	18 ± 2
PBAC-50	23 ± 5	16 ± 1	1039 ± 70	5 ± 0.3	39 ± 6
PBAC-60	46 ± 4	21 ± 1	1050 ± 25	8 ± 1	42 ± 1
PBAC-70	129 ± 12	31 ± 2	795 ± 60	16 ± 0.3	26 ± 1
PBAC-80	183 ± 22	38 ± 2	844 ± 19	19 ± 2	28 ± 2
PBAC-90	291 ± 28	43 ± 3	635 ± 37	27 ± 2	21 ± 1
PBAC-80-*mix*	52 ± 3	19 ± 1	1478 ± 46	6 ± 0.3	30 ± 1
PBAC-80-*cis*	166 ± 8	25 ± 1	682 ± 23	9 ± 0.2	14 ± 2
PBC	157 ± 7	17 ± 1	523 ± 7	14 ± 1	21 ± 1

[a] Tensile modulus E, tensile strength σ_t, elongation at break ε_b, yield stress σ_y and yield strain ε_y are determined by tensile testing.

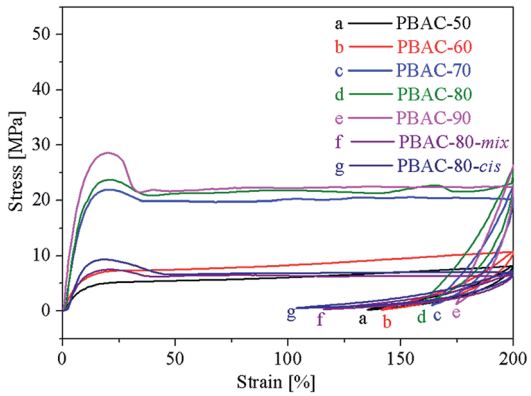

Fig. 7 Cyclic tensile testing strain–stress curves of PBAC copolymers.

strength as well as decreased ε_b like the hard segment does, but also initiates the transition of the copolymer from a semi-crystalline polymer to an amorphous one like the soft segment does.

Elastic properties of PBAC copolymers

Investigation on the elastic properties of PBAC copolymers further strengthens our point of view in the previous section. The elastic properties of PBAC copolymers along with PBA and PBC homopolymers are demonstrated by cyclic tensile testing. The shape recovery ratio at 200% strain in the first cycle of cyclic tensile testing is used to compare the elastic properties of PBAC copolymers. It is generally considered that a polymer with higher shape recovery ratio in the first cycle during the cyclic tensile testing tends to have better elastic property.[21,22,40,41]

The cyclic tensile testing strain–stress curves are shown in Fig. 7 and the shape recovery ratios at 200% strain during the first to five cycles are listed in Table 4. It can be seen from Table 4 that the recovery ratios of all samples increase with cycle numbers. Moreover, after the first so called training cycle, all samples have almost constant recovery ratios, which has also been reported by other researchers.[42,43] Actually, during the first cycle of the cyclic tensile test, the weak net-points or part of the crystalline regions are destructed and the molecular chains oriente in a more favorable way with regard to the direction of deformation. After the first cycle, an ideal orientated elastic network forms,[42] therefore, samples show higher recovery ratios of 90% after the second cycle.

In addition, both PBC and PBA homopolymers have poor elastic properties with shape recovery ratios at 200% strain in the first cycle ($R_r(1)$) of only ~10%. In the second place, addition of PBA to PBC and then increasing the PBA amount from 10 to 50%, the resulted PBAC copolymers have progressively increasing elastic properties with $R_r(1)$ improved from 13.6 all the way to 30.9%. These results provide solid evidence to support our previous opinion that PBA aliphatic chain unit resembles polyether soft segment. Finally, in regards to *cis*-CHDA, increasing its amount induces tremendous improvement in elastic property of PBAC copolymer. $R_r(1)$ increases from less than 20% to over 40 and 50% when *cis*-CHDA amount increases from 12 to 42 and 72% respectively. These results further reveal and demonstrate the soft characteristic of *cis*-CHDA.

Conclusions

PBAC copolymers are successfully obtained and the dependence of structure and properties of these copolymers on the composition as well as stereochemistry of CHDA are studied thoroughly. PBAC copolymer can be considered as triblock random copolymer consists with three parts: *trans*-PBC, *cis*-PBC and PBA. Neither *cis*-PBC nor PBA is crystallizable because *cis*-PBC contains only irregular *cis*-CHDA moiety which is unable to initiate crystallization and PBA unit length being too short. The *trans*-PBC part is the only crystallizable part and thus the thermal transitions such as melting and crystallization temperature of the PBAC copolymers actually origin from *trans*-PBC. The decreasing of the melting temperature of PBAC copolymer can be perfectly explained by the depression effect described with Flory equation, in which both the *cis*-PBC and PBA parts make contribution to the depression. Both parts are excluded from the *trans*-PBC crystalline region. In addition, *trans*-PBC is also responsible for both high modulus and strength and therefore acts as hard segment in PBAC copolymer. While amorphous PBA aliphatic unit functions like soft segment which leads to decreased melting temperature, thermal stability as well as modulus and strength, but increased elongation at break and shape recovery ratio. What's more

Table 4 Elastic properties of PBA, PBC and PBAC copolymers[a]

Sample	$R_r(1)$ (%)	$R_r(2)$ (%)	$R_r(3)$ (%)	$R_r(4)$ (%)	$R_r(5)$ (%)
PBA	10.4 ± 0.6	95.3 ± 0.2	97.6 ± 0.1	98.5 ± 0.2	98.6 ± 0.4
PBAC-50	30.9 ± 2.4	93.5 ± 0.1	97.0 ± 0.4	98.2 ± 0.2	98.2 ± 0.1
PBAC-60	29.9 ± 1.1	93.6 ± 0.3	97.1 ± 0.4	98.0 ± 0.3	98.6 ± 0.1
PBAC-70	17.8 ± 0.8	95.8 ± 0.4	97.6 ± 0.1	98.3 ± 0.1	98.7 ± 0.1
PBAC-80	19.6 ± 0.4	91.2 ± 0.6	96.3 ± 0.3	97.4 ± 0.2	98.4 ± 0.2
PBAC-90	13.6 ± 1.1	91.6 ± 1.1	96.2 ± 0.3	97.5 ± 0.5	98.0 ± 0.3
PBAC-80-*mix*	41.8 ± 0.4	93.5 ± 0.6	97.4 ± 1.0	98.0 ± 0.6	98.8 ± 0.4
PBAC-80-*cis*	50.5 ± 2.2	89.5 ± 0.5	95.1 ± 0.3	97.3 ± 1.2	97.5 ± 0.4
PBC	10.7 ± 0.5	94.7 ± 2.0	96.6 ± 0.7	99.6 ± 2.0	99.4 ± 1.1

[a] Elastic property is demonstrated by shape recovery ratio at 200% strain using cyclic tensile testing.

important, the special role that *cis*-CHDA plays in the PBAC copolymer is revealed for the first time. It shows effects of both hard and soft segment synchronously. It effectively suppresses the crystallization formed by *trans*-CHDA, which decreases the melting temperature of PBAC copolymers and finally turns PBAC copolymer from semicrystalline to amorphous, along with largely improved shape recovery ratio, just like what the soft segment would do. Therefore, form the viewpoint of the thermal properties, it plays a soft and rubbery role. Moreover, relatively high amount of *cis*-CHDA gives birth to PBAC copolymer with significantly improved modulus and strength, similar to the effect of a hard segment would display. Accordingly, from the viewpoint of the modulus and strength, it is rigid, especially compared with the aliphatic PBA part. In conclusion, we have exposed both the rigid and soft roles of *cis*-CHDA it plays in a copolyester system. Other types of polymers such as polyamide, polycarbonate as well as polyurethane can also take advantage of this moiety, so that they would show interesting and tunable properties.

Experimental

Materials

1,4-Butanediol (BDO) (99%), adipic acid (AA) (AR, 99%), titanium(IV) butoxide (99%) and antioxidant 1010 (95%) were all purchased from Aladdin Reagent Co. Ltd (Shanghai, China). Chloroform (HPLC) was obtained from Sinopharm Chemical Reagent Co., Ltd (Shanghai, China). *trans*-1,4-Cyclohexanedicarboxylic acid (*trans*-CHDA) (99%) and *mix*-1,4-cyclohexanedicarboxylic acid (*mix*-CHDA) with a cis/trans ratio of 50/50 were purchased from Nanjing Chemlin Chemical Industry Co., Ltd. *cis*-CHDA (97%) was obtained by separation and purification of *mix*-CHDA from ethanol according to methods described in the literature.[44,45] All the chemicals are used as received without further treatment.

Synthesis of PBAC copolymers

PBAC copolymers are prepared *via* a two-step melt polycondensation process. In the first step, two esterification products *i.e.* bis(hydroxylbuthylene) adipate (BHBA) and bis(hydroxylbuthylene) 1,4-cyclohexandicarboxylate (BHBC) are respectively obtained by esterification reaction between BDO with AA and CHDA. In the second step, BHBA and BHBC are then used for the synthesis of PBAC final products *via* polycondensation reaction. A series of PBAC copolymers with different compositions are produced by simple changing the feeding ratio of BHBA and BHBC in the second step. The following describes the detailed process for the synthesis of PBAC copolymer (Scheme 2).

For the synthesis of BHBA, AA (292.0 g), BDO (306.0 g) and the catalyst (titanium(IV) butoxide, 1.5 g, 0.05 wt% of AA) were added to a 1 L autoclave. The mixture was placed under vacuum (0.1 kPa) and then purged with N_2 gas. This cycle was repeated for three times. Subsequently, the mixture was heated to 230 °C under N_2 until the amount of the distilled water reached 80% of its theoretic amount (typically 4 h). The system was then evacuated below 100 Pa to remove the extra amount of BDO. BHBC was prepared with similar procedure using CHDA as starting material, and the reaction temperature was 200 °C. Both BHBA and BHBC were obtained as white waxy solid and were dried in 50 °C under vacuum overnight and then kept in a desiccator before use.

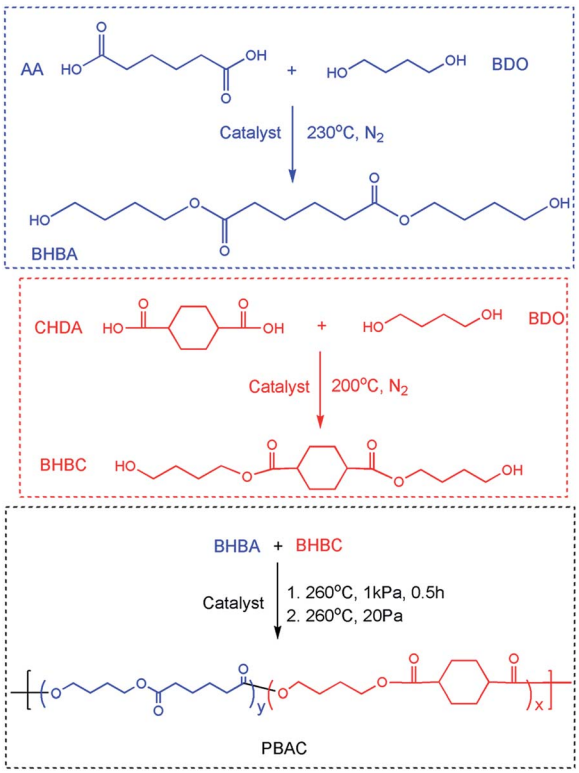

Scheme 2 Synthesis of PBAC copolymer.

For the synthesis of PBAC copolymer, the process for the synthesis of PBAC copolymer with 50 mol% of PBC is described here as an example. BHBA (230 g) and BHBC (130 g) were added to a 1 L autoclave with catalyst (titanium(IV) butoxide, 0.09 g, 0.025 wt% of BHBA and BHBC) and antioxidant 1010 (0.054 g, 0.015 wt% of BHBA and BHBC). The mixture was placed under vacuum (0.1 kPa) and then purged with N_2 gas. This cycle was repeated for three times. Subsequently, the system was sealed and evacuated to 1 kPa, and heated up to 260 °C and maintained for 0.5 h, after which, the system was subject to higher vacuum (below 20 Pa) for about 3–5 h to get high molecular weight products. All resulted polymers were used without further treatment.

Characterization

Molecular weights and molecular weight distributions were measured on PL-GPC220 high temperature gel permeation chromatography (GPC) equipped with a PLgel – 5 μm MIXED-D column with a dimension of 300 × 7.5 mm and a refractive index detector. HPLC grade chloroform was used as elution solvent at 40 °C with a flow rate of 1.0 mL min^{-1} and molecular

weight was calibrated with polystyrene standard. The concentration of all samples was 20 mg/3 mL.

Structure and *cis*/*trans* ratio of 1,4-cyclohexylene ring in the polymer chain of PBC were determined by proton and carbon 13 nuclear magnetic resonance (^{1}H NMR and ^{13}C NMR) in $CDCl_3$ solvent using a Bruker AVIII400 NMR spectrometer at room temperature.

Differential scanning calorimetry (DSC) measurements were performed using differential scanning calorimeter (METTLER-TOLEDO DSC I). Temperature calibaration was carried out using an indium standard. Measurements were performed under a nitrogen atmosphere at a flow rate of 50 mL min^{-1}. About 5 mg of sample was placed in an alumina sample pan and the measurement was carried out according to the following process: the sample was heated up to 260 °C at 10 °C min and held at this temperature for 4 min to erase the heat history. It was then cooled down to −40 °C at 10 °C min. Subsequently, a second heating scan was performed at 10 °C min to 260 °C. The melting point (T_m) and heat of fusion (ΔH_m) were obtained from the second heating scan and the crystallization temperature (T_c) was taken from the cooling scan. The degree of crystallinity was calculated according to the following equation:

$$\chi_c(\%) = \frac{\Delta H_m}{f(\text{PBA}) \times \Delta H_m^\theta(\text{PBA}) + f(\textit{trans}\text{-PBC}) \times \Delta H_m^\theta(\textit{trans}\text{-PBC})} \times 100\%$$

where χ_c is the degree of crystallinity, f is the weight fraction, ΔH_m is the experimental melting heat of fusion, and ΔH_m^θ is the heat of fusion of 100% crystalline (135 J g^{-1} for PBA[36] and 141 J g^{-1} for *trans*-PBC calculated according to the group contribution theory).[46,47]

Thermal stability measurements were conducted using a Mettler-Toledo TGA/DSC thermogravimetric analysis (TGA). For each sample, 6–10 mg sample was placed in a ceramic furnace and the TGA curve was recorded ranging from 50 to 800 °C with a heating rate of 10 °C min^{-1} under dry nitrogen or air atmosphere with a flow rate of 50 mL min^{-1}. We took the temperature at which the weight loss was 5% ($T_{5\%}$) as an index to evaluate the thermal stability of the sample.

Wide angle X-ray diffraction (WAXD) patterns were performed on a D8 Advance diffractometer (Bruker AX, Germany) with a Cu Kα radiation (λ = 0.154 nm). The equipment was operated at 40 kV and 40 mA under room temperature. The sample films were scanned in fixed time mode with 9 min under diffraction angle 2θ in the range of 5–50°.

Tensile testing was performed in an Instron 5567 tensile testing machine with a 500 N load cell. The stretching rate was 100 mm min^{-1} and the test temperature was 25 °C. Dumb-bell-shaped sample bars with dimensions of 35.0 mm (length), 2.0 mm (neck width) and 0.5 mm (thickness) were prepared by press-molding at temperature 20 °C higher than T_m or T_f of the sample and subsequently cooled down to temperature below its T_c or simply to room temperature, without releasing the pressure. All data were obtained by averaging the data from five parallel measurements.

Cyclic tensile testing was done with an Instron 5567 apparatus. The dumb-bell-shaped sample bars with dimensions of 35.0 mm (length), 2.0 mm (width), and 0.5 mm (thickness) were stretched to ε_m, 200% elongation at room temperature with a 100 mm min^{-1} stretching rate. Then the clamps began to return with a speed of 50 mm min^{-1} until the force on the sample was 0. After the above two steps, one cycle is complete. Three samples were tested to calculate mean values and standard deviation. Every sample was subjected to 5 cycles and the shape recovery rate (R_r) was calculated according to the following equation:

$$R_r(N) = \frac{\varepsilon_m - \varepsilon_p(N)}{\varepsilon_m - \varepsilon_p(N-1)}$$

where N is the cycle number, ε_m is the maximum strain imposed on the material, $\varepsilon_p(N)$ and $\varepsilon_p(N-1)$ are the strains of the sample in two successive cycles when the force on the sample is 0 and $R_r(N)$ is based on two successive cycles.

Acknowledgements

The authors are grateful for the financial support by the National Natural Science Foundation of China (NSFC, Grant No. 51503217), Key Projects in the National Science & Technology Pillar Program of China (2015BAD15B08), and Ningbo Innovation Project (Grant No. 2015B11003).

Notes and references

1 D. J. Brunelle and T. Jang, *Polymer*, 2006, **47**, 4094–4104.
2 C. Berti, E. Binassi, A. Celli, M. Colonna, M. Fiorini, P. Marchese, E. Marianucci, M. Gazzano, F. D. I. Credico and D. J. Brunelle, *J. Polym. Sci., Part B: Polym. Phys.*, 2008, **46**, 619–630.
3 C. Berti, A. Celli, P. Marchese, G. Barbiroli, F. Di Credico, V. Verney and S. Commereuc, *Eur. Polym. J.*, 2009, **45**, 2402–2412.
4 M. Gigli, N. Lotti, M. Gazzano, V. Siracusa, L. Finelli, A. Munari and M. Dalla Rosa, *Ind. Eng. Chem. Res.*, 2013, **52**, 12876–12886.
5 M. Gigli, N. Lotti, M. Vercellino, L. Visai and A. Munari, *Mater. Sci. Eng., C*, 2014, **34**, 86–97.
6 W. J. Yoon, K. S. Oh, J. M. Koo, J. R. Kim, K. J. Lee and S. S. Im, *Macromolecules*, 2013, **46**, 2930–2940.
7 L. Genovese, N. Lotti, M. Gazzano, L. Finelli and A. Munari, *eXPRESS Polym. Lett.*, 2015, **9**, 972–983.
8 J. M. Dennis, J. S. Enokida and T. E. Long, *Macromolecules*, 2015, **48**, 8733–8737.
9 B. Vanhaecht, M. N. Teerenstra, D. R. Suwier, R. Willem, M. Biesemans and C. O. R. E. Koning, *J. Polym. Sci., Part A: Polym. Chem.*, 2001, **39**, 833–840.
10 J. Liu and A. F. Yee, *Macromolecules*, 1998, **31**, 7865–7870.
11 L. Wang, Z. Xie, X. Bi, X. Wang, A. Zhang, Z. Chen, J. Zhou and Z. Feng, *Polym. Degrad. Stab.*, 2006, **91**, 2220–2228.
12 M. Fabbri, M. Soccio, M. Gigli, G. Guidotti, R. Gamberini, M. Gazzano, V. Siracusa, B. Rimini, N. Lotti and A. Munari, *Polymer*, 2016, **83**, 154–161.

13 L. Genovese, M. Soccio, M. Gigli, N. Lotti, M. Gazzano, V. Siracusa and A. Munari, *RSC Adv.*, 2016, **6**, 55331–55342.
14 Y. Gong, C. W. Hu, H. Li, K. L. Huang and W. Tang, *J. Solid State Chem.*, 2005, **178**, 3152–3158.
15 L. P. Chen, A. F. Yee, J. M. Goetz and J. Schaefer, *Macromolecules*, 1998, **31**, 5371–5382.
16 C. Berti, A. Celli, P. Marchese, E. Marianucci, G. Barbiroli and F. Di Credico, *Macromol. Chem. Phys.*, 2008, **209**, 1333–1344.
17 H. R. Kricheldorf and G. Schwarz, *Makromol. Chem.*, 1987, **188**, 1281–1294.
18 N. Sánchez-Arrieta, A. M. de Ilarduya, A. Alla and S. Muñoz-Guerra, *Eur. Polym. J.*, 2005, **41**, 1493–1501.
19 M. Gigli, N. Lotti, M. Gazzano, V. Siracusa, L. Finelli, A. Munari and M. D. Rosa, *Polym. Degrad. Stab.*, 2014, **105**, 96–106.
20 T. E. Sandhya, C. Ramesh and S. Sivaram, *Macromolecules*, 2007, **40**, 6906–6915.
21 F. Liu, J. Zhang, J. Wang, H. Na and J. Zhu, *RSC Adv.*, 2015, **5**, 94091–94098.
22 F. Liu, J. Zhang, J. Wang, X. Liu, R. Zhang, G. Hu, H. Na and J. Zhu, *J. Mater. Chem. A*, 2015, **3**, 13637–13641.
23 C. Berti, A. Celli, P. Marchese, E. Marianucci, S. Sullalti and G. Barbiroli, *Macromol. Chem. Phys.*, 2010, **211**, 1559–1571.
24 Z. Wei, C. Zhou, Y. Yu and Y. Li, *RSC Adv.*, 2015, **5**, 42777–42788.
25 M. Vert, *Biomacromolecules*, 2005, **6**, 538–546.
26 V. Tserki, P. Matzinos, E. Pavlidou, D. Vachliotis and C. Panayiotou, *Polym. Degrad. Stab.*, 2006, **91**, 367–376.
27 S. Y. Hwang, X. Y. Jin, E. S. Yoo and S. S. Im, *Polymer*, 2011, **52**, 2784–2791.
28 G. C. Liu, J. B. Zeng, C. L. Huang, L. Jiao, X. L. Wang and Y. Z. Wang, *Ind. Eng. Chem. Res.*, 2013, **52**, 1591–1599.
29 G. Wang and Z. Qiu, *Ind. Eng. Chem. Res.*, 2012, **51**, 16369–16376.
30 M. S. Nikolic and J. Djonlagic, *Polym. Degrad. Stab.*, 2001, **74**, 263–270.
31 X. Q. Shi, H. Ito and T. Kikutani, *Polymer*, 2005, **46**, 11442–11450.
32 E. Cranston, J. Kawada, S. Raymond, F. G. Morin and R. H. Marchessault, *Biomacromolecules*, 2003, **4**, 995–999.
33 L. Wu, R. Mincheva, Y. Xu, J.-M. Raquez and P. Dubois, *Biomacromolecules*, 2012, **13**, 2973–2981.
34 B. Wu, Y. Xu, Z. Bu, L. Wu, B.-G. Li and P. Dubois, *Polymer*, 2014, **55**, 3648–3655.
35 R. Herrera, L. Franco, A. Rodríguez-Galán and J. Puiggalí, *J. Polym. Sci., Part A: Polym. Chem.*, 2002, **40**, 4141–4157.
36 J. Yang, Y. Chen, S. Qin, J. Liu, C. Bi, R. Liang, T. Dong and X. Feng, *Ind. Eng. Chem. Res.*, 2015, **54**, 8048–8055.
37 Z. Gan, K. Kuwabara, H. Abe, T. Iwata and Y. Doi, *Biomacromolecules*, 2004, **5**, 371–378.
38 M. Yokouchi, Y. Sakakibara, Y. Chatani, H. Tadokoro and T. Tanaka, *Macromolecules*, 1975, **9**, 266–273.
39 J. Zhang, F. Liu, J. Wang, H. Na and J. Zhu, *Chin. J. Polym. Sci.*, 2015, **33**, 1283–1293.
40 R. M. Versteegen, R. P. Sijbesma and E. W. Meijer, *Macromolecules*, 2005, **38**, 3176–3184.
41 C. L. Lewis, Y. Meng and M. Anthamatten, *Macromolecules*, 2015, 150715075734002.
42 L. Zhang, Y. Jiang, Z. Xiong, X. Liu, H. Na, R. Zhang and J. Zhu, *J. Mater. Chem. A*, 2013, **1**, 3263.
43 P. Ping, W. Wang, X. Chen and X. Jing, *J. Polym. Sci., Part B: Polym. Phys.*, 2007, **45**, 557–570.
44 B. Vanhaecht, B. Rimez, R. Willem, M. Biesemans and C. E. Koning, *J. Polym. Sci., Part A: Polym. Chem.*, 2002, **40**, 1962–1971.
45 M. A. Osman, *Macromolecules*, 1986, **19**, 1824–1827.
46 Y. H. Park and C. G. Cho, *J. Appl. Polym. Sci.*, 2001, **79**, 2067–2075.
47 K. G. Joback and R. C. Reid, *Chem. Eng. Commun.*, 1987, **57**, 233–243.